



# Radiologic and Histopathologic Correlation of Different Growth Patterns of Metastatic Uveal Melanoma to the Liver

Albert Liao, BA,<sup>1</sup> Pardeep Mittal, MD,<sup>2</sup> David H. Lawson, MD,<sup>3</sup> Jenny J. Yang, PhD,<sup>4</sup> Eszter Szalai, MD, PhD,<sup>1</sup> Hans E. Grossniklaus, MD<sup>1,5</sup>

**Purpose:** The purpose of this study was to correlate magnetic resonance imaging (MRI) radiographic results with histopathologic growth patterns of metastatic uveal melanoma (UM) to the liver.

**Design:** Clinicopathologic correlation.

**Participants:** Patients with metastatic UM to the liver.

**Methods:** A retrospective review of MRI images of patients with metastatic UM to the liver at a single institution between 2004 and 2016 was performed. The MRI growth patterns were classified as nodular or diffuse. The histopathologic findings of core liver biopsies of liver metastases identified by needle localization in a subset of these patients were reviewed. The core samples were evaluated by routine light microscopy, including immunohistochemical/immunofluorescent staining for CD31, CD105, and HMB45, and classified as exhibiting an infiltrative or nodular growth pattern.

**Main Outcome Measures:** Magnetic resonance images and core biopsy findings.

**Results:** A total of 32 patients were identified with metastatic UM to the liver that was imaged by MRI, and 127 lesions were identified. A total of 46 lesions were classified by MRI as infiltrative and 81 as nodular. There were 9 needle-localized core biopsies that corresponded to MRI of metastatic lesions. Of these 9 lesions, 3 that were classified as infiltrative on MRI exhibited stage I infiltrative histologic growth patterns; of the remaining 6 that were classified as nodular by MRI, 5 histologically demonstrated stage II or stage III infiltrative growth patterns and 1 histologically demonstrated a nodular growth pattern.

**Conclusions:** Magnetic resonance imaging of hepatic infiltrative growth patterns of metastatic UM corresponded to stage I histologic infiltrative growth in the sinusoidal spaces, whereas MRI nodular growth patterns corresponded to stage II/III histologic infiltrative growth that replaced the hepatic lobule or histologic nodular growth in the portal triad that effaced adjacent hepatic parenchyma. *Ophthalmology* 2017;■:1–9 © 2017 by the American Academy of Ophthalmology



Supplemental material available at [www.aaojournal.org](http://www.aaojournal.org).

Uveal melanoma (UM) is the most common primary intraocular malignancy in adults.<sup>1</sup> Uveal melanoma accounts for 3.7% of all reported melanoma cases in the United States,<sup>2</sup> and its mean age-adjusted incidence is approximately 5.1 per million.<sup>3</sup> Current treatment methods for UM include transpupillary thermotherapy, brachytherapy, proton beam irradiation, local resection, and enucleation.<sup>4,5</sup> Despite the development of effective local therapies, the 5-year survival rate for patients with UM has not changed over the past 3 decades, remaining at approximately 80%. This can partially be attributed to the high rate of metastasis in these patients (~50%) coupled with the fact that there is no effective adjuvant therapy.<sup>6,7</sup> The 1-year survival rate for patients with metastatic UM is approximately 15%, with reported median survivals ranging from 4 to 15 months.<sup>8</sup>

The liver is the most common site of metastasis for UM; it is the initially detected metastatic site in more than 60% of patients.<sup>9</sup> Hepatic metastases are present in more than 90% of patients with metastatic disease.<sup>10</sup> It is important to

understand the growth characteristics of UM in the liver with regard to diagnosis and therapy. Our laboratory has characterized the existence of 2 distinct histologic growth patterns of metastatic UM in the liver.<sup>11</sup> The lobular or infiltrative pattern refers to tumor infiltration directly into the hepatic lobules that is accompanied by perlobular septal fibrosis. The portal or nodular pattern describes distinct clusters of tumor cells located around the portal venules in the portal triad that push aside, or “efface,” the neighboring liver parenchyma. In the infiltrative pattern, tumor cells receive their nutrition from blood in the sinusoidal or pseudosinusoidal spaces, and there is minimal angiogenesis.<sup>12</sup> In the nodular pattern, the tumor coopts adjacent portal venules and exhibits angiogenesis as the metastatic focus enlarges, and new tumor blood vessels extend from branches of the hepatic arteriole.<sup>11,12</sup>

Several radiographic studies have also identified differential growth patterns of metastatic UM in the liver; identification of these growth patterns has important clinical

implications. For example, tumors with a radiographic nodular growth pattern on angiography appear to be more responsive to chemoembolization or radioembolization compared with tumors classified with a radiographic infiltrative pattern.<sup>13–15</sup> Until now, the relationship between these radiographic and histopathologic growth patterns has not been explored. In this study, we evaluated the magnetic resonance imaging (MRI) features of metastatic UM to the liver and correlated findings with histopathologic patterns from biopsies.

## Methods

We retrospectively evaluated all patients diagnosed with hepatic metastases from malignant melanoma of the choroid who had sequential imaging performed at Emory University from January 1, 2004, to September 1, 2016. This study was approved by the Emory University School of Medicine Institutional Review Board (Atlanta, GA). Our protocol for imaging is described in [Table S1](#) (available at [www.aaojournal.org](http://www.aaojournal.org)). Visceral metastases from melanoma have a wide variety of appearances on MRI. The pattern of tumor vascularity is exploited for detection of liver metastases in gadolinium chelate-enhanced MRI.<sup>16</sup> Hypervascular liver metastases are usually from primary tumors, such as melanoma and neuroendocrine tumors, including carcinoid, islet cell tumors, renal cell carcinoma, and thyroid carcinoma. These hypervascular metastases show peak enhancement in hepatic arterial phase and were obtained 20 seconds after contrast injection as fat-suppressed T1-weighted images. The imaging appearance of liver metastases on portal venous and delayed phases can be variable, and images were acquired 70 and 180 seconds after contrast injection, respectively, as fat-suppressed T1-weighted images. Because UM metastatic lesion scans show high T1 signal on noncontrast images because of the presence of melanin ([Fig 1](#)), it can be challenging to determine enhancement after contrast; therefore, subtraction images were used.<sup>17</sup> Liver metastases from melanoma may also show transient peripheral rim enhancement in the arterial phase<sup>18</sup> ([Fig 2](#)). Our institution preferentially uses MRI for liver imaging because of its superior soft-tissue contrast and lack of ionizing radiation, because these patients require frequent follow-ups to assess treatment response.

An experienced radiologist (P.M.) assessed the radiographic images. Patients' core biopsy samples, if available, were matched with the radiographic biopsy site. This was performed by reviewing patient biopsy reports and visualizing the core needle entering the lesion in question on MRI and computed tomography (CT). For each of these cases, sections of the core liver biopsies with suspected metastasis were obtained and reviewed by an experienced pathologist (H.E.G.). Patient samples were pseudoanonymized for data other than age and sex. All biopsy samples were routinely processed and stained with hematoxylin–eosin, Masson trichrome, and reticulin. Immunohistochemical staining using CD31 (DAKO, Carpinteria, CA; 1:180) was used to evaluate for the presence of vascular channels (CD31+), and immunofluorescence staining for CD105 (DAKO; 1:5) was used to identify new vascular endothelium (CD105+). Immunohistochemical stains for HMB45 (DAKO; 1:50) were used to confirm the melanoma. CD31 stains mature vascular endothelium.<sup>19</sup> CD105 is a transforming growth factor- $\beta$  receptor expressed in embryonic endothelial cells; its presence indicates angiogenesis.<sup>20</sup> The slides stained with hematoxylin–eosin, Masson trichrome, and immunohistochemical were examined by light microscopy to determine the presence and histologic growth pattern of the metastases (nodular or infiltrative), as previously

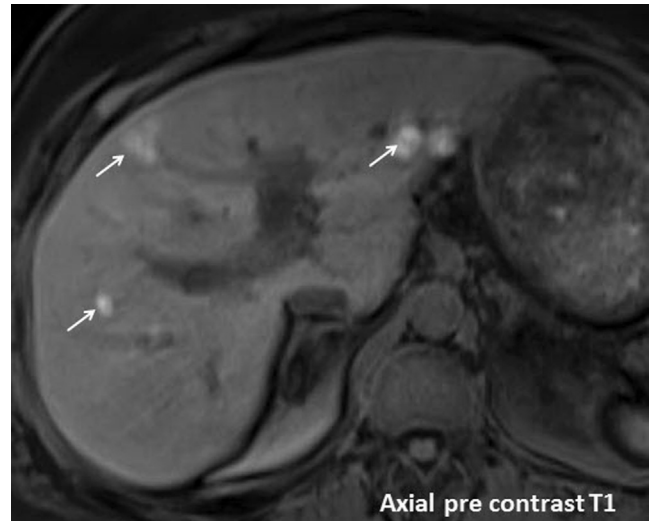


**Figure 1.** Metastatic uveal melanoma in the liver with high T1 signal. T1 axial image through the liver demonstrates multiple foci of hyperintensity involving both lobes of the liver as the result of melanin (arrows).

described.<sup>11,12</sup> The radiographic features were evaluated in a masked fashion and then compared with the corresponding histologic growth patterns.

## Results

We identified 32 patients who were diagnosed with metastatic UM and had hepatic imaging. The average age of the patients was 58.5 years, and there were 21 male and 11 female patients. The treatments for the primary tumors in these patients were brachytherapy with an iodine-125 plaque in 16 patients, enucleation in 13 patients, external beam radiation in 1 patient, subsequent enucleation after plaque failure in 1 patient, and plaque therapy with laser photocoagulation in 1 patient. The metastatic disease was treated as follows: chemotherapy or chemoimmunotherapy was administered to 14 patients; 1 patient received radioablation; 1 patient had a resection as the sole treatment; 8 patients had a combination of chemotherapy/chemoimmunotherapy/embolization; 1 patient had laser ablation/chemoimmunotherapy; 1 patient had radiation/chemoimmunotherapy; 2 patients had only embolization; 1 patient had no treatment; and 3 patients did not have treatment records available. A total of 127 lesions were followed radiographically from this patient population.

Classically, UM metastases may reveal a hyperintense signal on unenhanced T1-weighted MRI due to the paramagnetic effect of melanin, which is present in the minority of cases. More commonly, lesions were hypointense or isointense on T1-weighted sequences and hyperintense on T2-weighted sequences. Two predominant patterns were seen on MRI. The MRI infiltrative pattern shown in [Figure 3](#) was characterized as an enlarged, extensive heterogeneous enhancement of the liver that does not respect the liver lobule boundaries and had no distinct nodularity. The MRI nodular pattern, shown in [Figure 4](#), consisted of multiple hyperenhancing lesions in the liver with defined boundaries that were distinct from the surrounding parenchyma. In total, 46 lesions were classified as infiltrative on imaging and 81 lesions were classified as nodular on imaging. Twelve patients had both infiltrative and nodular lesions on imaging.

We had access to core biopsy pathology samples for 9 patients. Three of these 9 patients had biopsies from lesions that

Download English Version:

<https://daneshyari.com/en/article/8794066>

Download Persian Version:

<https://daneshyari.com/article/8794066>

[Daneshyari.com](https://daneshyari.com)